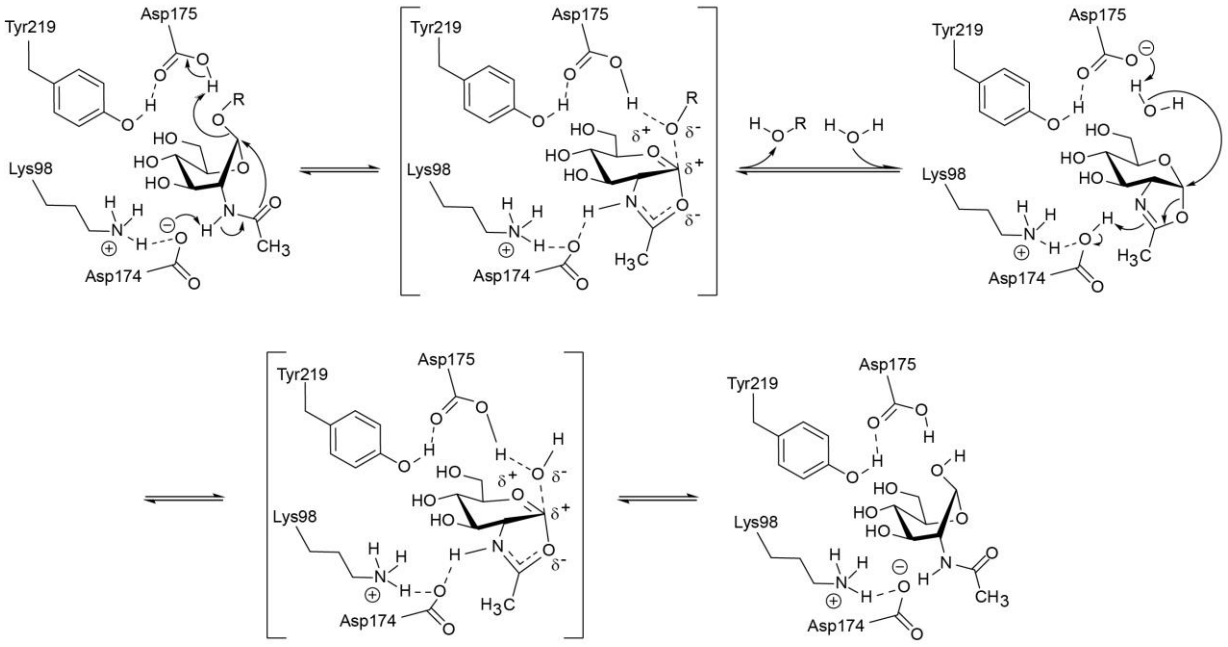

Supplementary Figure 1

Substrate-assisted mechanism of OGA.

OGA-catalyzed hydrolysis of O-GlcNAcylation via a substrate-assisted mechanism, adapted from a previous report (Dennis, R. J. *et al.*, *Nat. Struct. Mol. Biol.* **13,** 365–371, 2006). The roles of ancillary residues Lys98 and Tyr219 are inferred from the crystal structure of OGA_{cryst}–thiamet-G from this study.

a

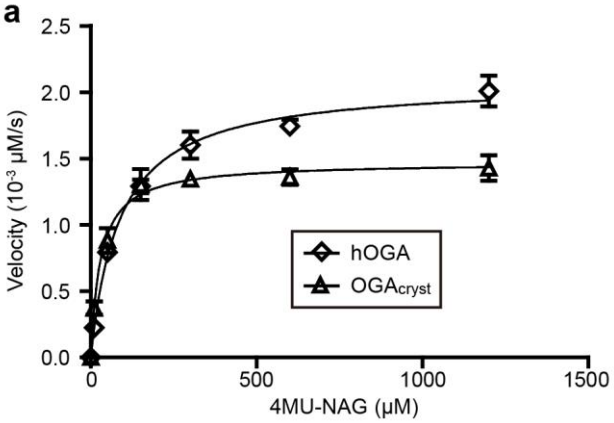

b

Kinetic constants	hOGA	OGA_{cryst}
K_m (µM 4MU-NAG)	87.57 ± 6.91	29.68 ± 3.37
k_{cat} (min^{-1})	62.35 ± 0.02	44.09 ± 0.02
k_{cat} / K_m (min^{-1} μM^{-1})	0.71 ± 0.06	1.48 ± 0.19

Supplementary Figure 2

Kinetic parameters of hOGA and OGA_{cryst} proteins.

(**a**) Michaelis–Menten plots of hOGA and OGA_{cryst} with varying concentrations of 4MU-NAG. Data were fitted using GraphPad Prism. Error bars represent s.d. values derived from three independent experiments. (**b**) Summary of the kinetic parameters of hOGA and OGA_{cryst}. The K_m and k_{cat} were determined from three independent experiments and displayed as average ± s.d..

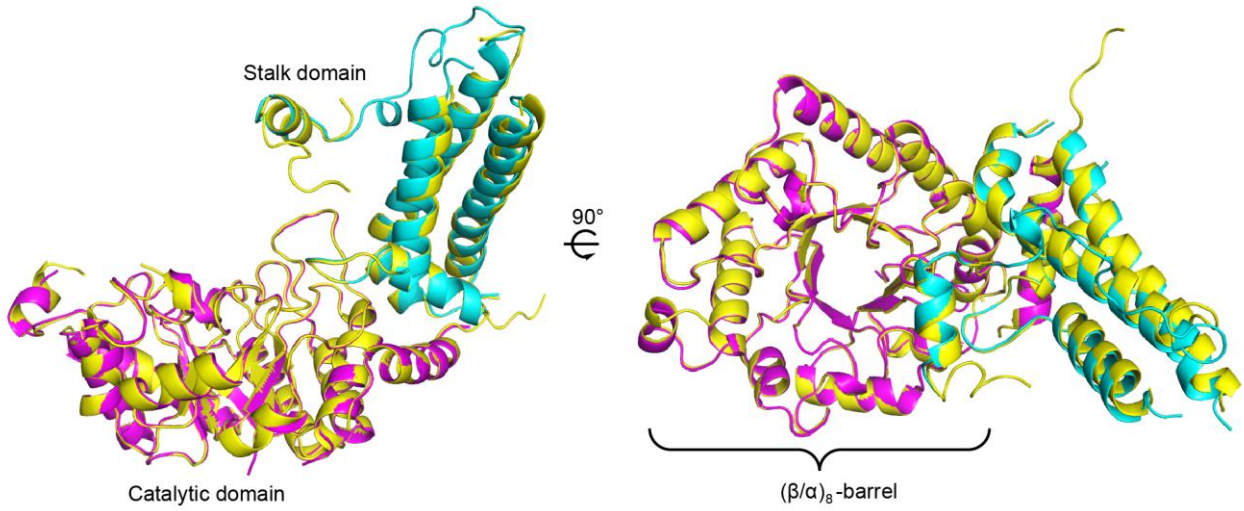

Supplementary Figure 3

Structural comparison of the two sister monomers of OGA_{cryst}.

Two perpendicular views of superimposed OGAα and OGAβ reveal that the catalytic domains are folded into an identical $(\beta/\alpha)_8$-barrel, while the stalk domains display a slight variation. OGAα is colored yellow; the catalytic domain and stalk domain of OGAβ are colored magenta and cyan, respectively.

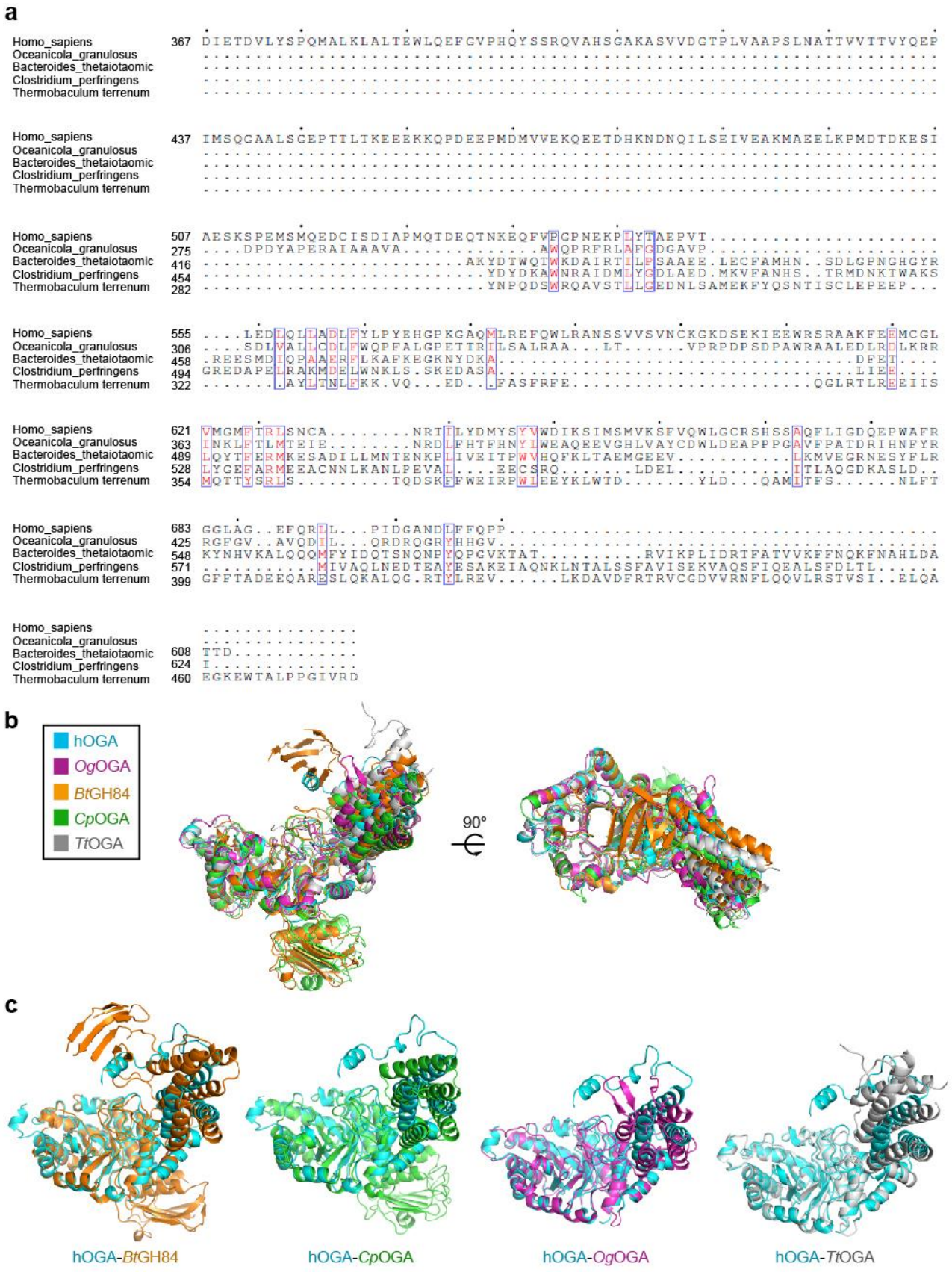
a
Homo_sapiens
Oceanicola_granulosus
Bacteroides_thetaiotaomic
Clostridium_perfringens
Thermobaculum terrenum
b
hOGA
OgOGA
BtGH84
CpOGA
TtOGA
90°
c
hOGA-BtGH84
hOGA-CpOGA
hOGA-OgOGA
hOGA-TtOGA

Supplementary Figure 4

The sequence and structure of the hOGA stalk domain are markedly different from those of its bacterial homologs.

(**a**) Sequence alignment and (**b**-**c**) structural comparison of the stalk domains of OGA proteins from human (hOGA, cyan) and representative bacterial species: *Oceanicola granulosus* (*Og*OGA, PDB: 2XSA, magenta) (Schimpl, M. *et al*., *Biochem. J.* **432,** 1–7, 2010), *Bacteroides thetaiotaomicron* (*Bt*GH84, PDB: 2CHO, orange) (Dennis, R. J. *et al.*, *Nat. Struct. Mol. Biol.* **13,** 365–371, 2006), *Clostridium perfringens* (*Cp*OGA, PDB: 2CBJ, green) (Rao, F. V. *et al.*, *EMBO J.* **25,** 1569–1578, 2006) and *Thermobaculum terrenum* (*Tt*OGA, PDB: 5DIY, grey) (Ostrowski, A., *et al*., *J. Biol. Chem.* **290,** 30291–30305, 2015). In the sequence alignment, variable and similar residues are shown in black and red, respectively.

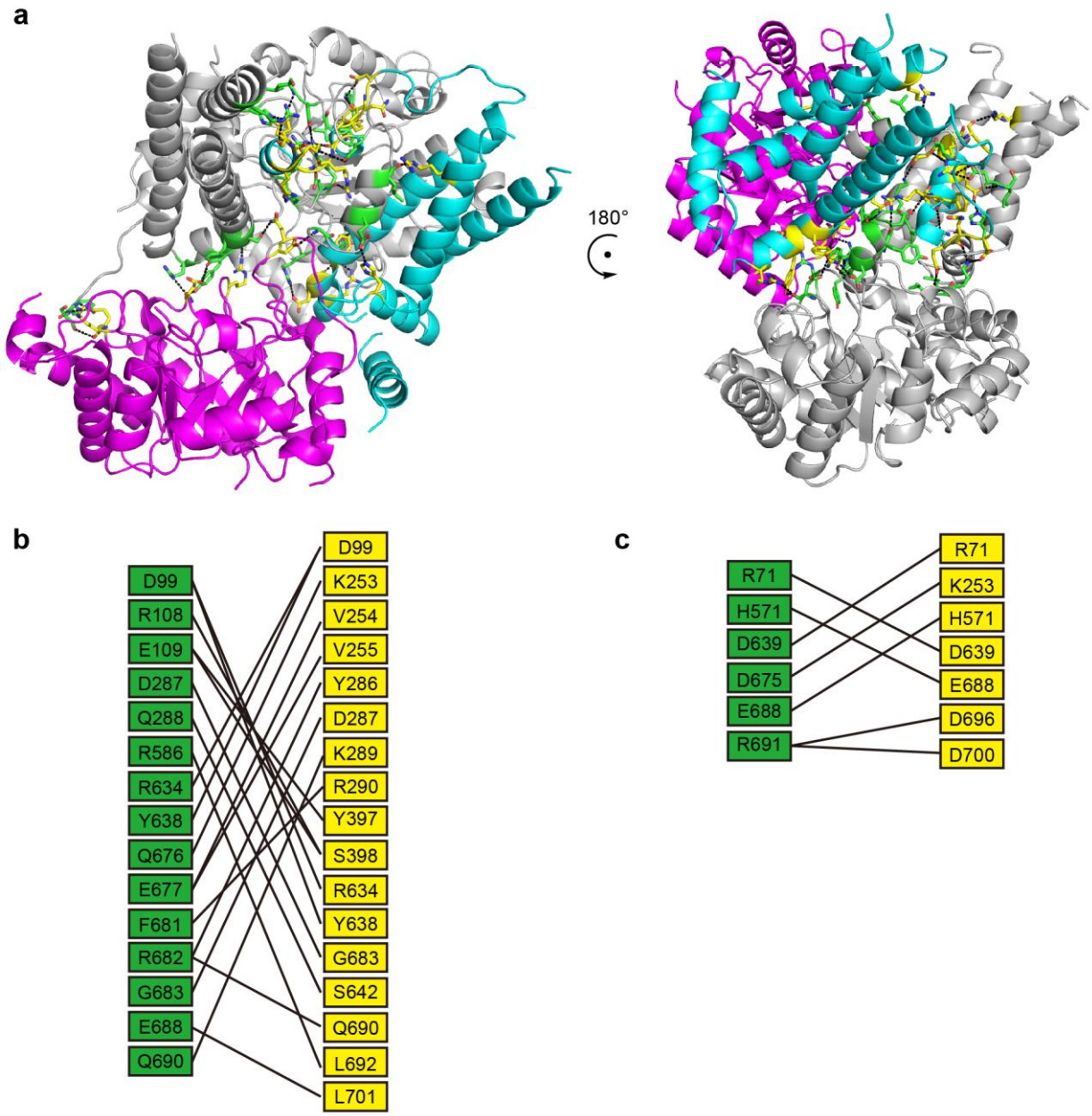

Supplementary Figure 5

Extensive polar interactions stabilize the dimerization of OGA_{cryst}.

(**a**) Two different views of OGA_{cryst} with dimerization interface. OGAα is colored gray; the catalytic domain and stalk domain of OGAβ are colored magenta and cyan, respectively. (**b**) Schematic representation of the hydrogen bonds detected at the dimerization interface. (**c**) Schematic representation of the salt bridges detected at the dimerization interface. Residues from OGAα and OGAβ participating in the polar interactions are colored in yellow and green, respectively.

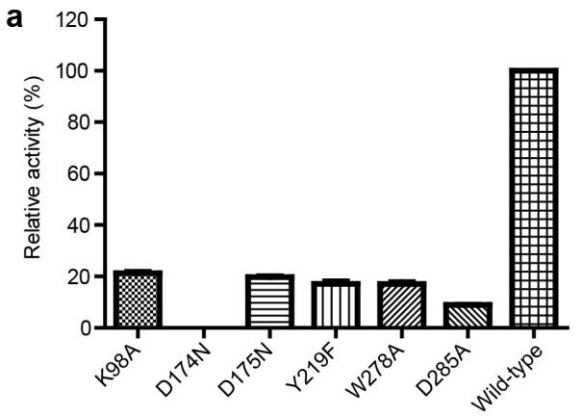

b

Kinetic constants	K_m' (μM p53 glycopeptide)
OGA_{cryst}	796.20 ± 57.04
Wild-type	819.10 ± 68.46
Wild-type	(2534.00 ± 265.30)*
F223A	3840.00 ± 86.26
W679A	2639.00 ± 116.10

Supplementary Figure 6

Relative activities and substrate-binding evaluation of hOGA variants.

(**a**) The activities of hOGA mutants were measured using 4MU-NAG and normalized to the wild-type enzyme. The error bars represent the s.d. values derived from three independent experiments. (**b**) To evaluate the contribution of hydrophobic interactions with the p53 glycopeptide (Ac-QLWVD*S*(O-GlcNAc)TPPPG), the Michaelis constants of hOGA and mutants were determined using 4MU-NAG as the reporter substrate following multisubstrate enzyme kinetics as shown previously (Schimpl, M. *et al*., *Biochem. J.* **432,** 1–7, 2010; Schimpl, M. *et al*., *Chem. Biol.* **19,** 173–178, 2012; Xie, D. *et al*., *Protein Science* **8,** 2460–2464, 1999). *The Michaelis constant of wild-type hOGA was measured towards a W(-3)A mutant of p53 glycopeptide (Ac-QL**A**VD*S*(O-GlcNAc)TPPPG) using a similar assay. The K_{m}' values were determined from three independent experiments and displayed as average ± s.d..

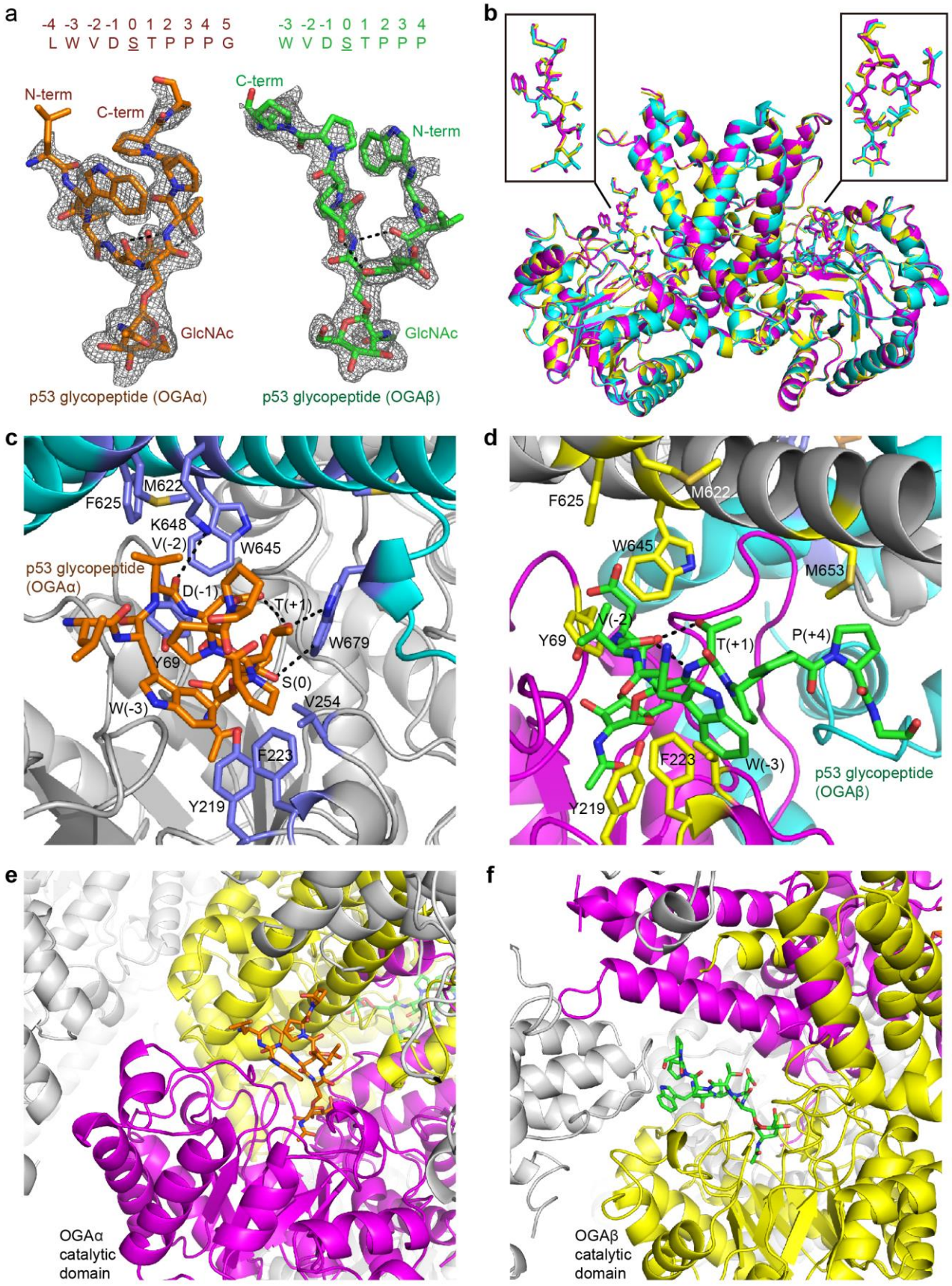
a
-4 -3 -2 -1 0 1 2 3 4 5
L W V D S T P P P G
-3 -2 -1 0 1 2 3 4
W V D S T P P P
N-term
C-term
GlcNAc
C-term
N-term
GlcNAc
p53 glycopeptide (OGAα)
p53 glycopeptide (OGAβ)
b
c
F625
M622
K648
V(-2)
W645
p53 glycopeptide
(OGAα)
D(-1)
T(+1)
W679
Y69
S(0)
W(-3)
V254
F223
Y219
d
F625
M622
W645
M653
V(-2)
Y69
T(+1)
P(+4)
F223
W(-3)
p53 glycopeptide
(OGAβ)
Y219
e
OGAα
catalytic
domain
f
OGAβ
catalytic
domain

Supplementary Figure 7

Binding conformation of p53 glycopeptides in the OGA_{cryst}–p53 complex.

(**a**) *Fo–Fc* difference map of p53 glycopeptides from the OGA_{cryst}–p53 complex (contoured at 3σ). The peptides from OGAα and OGAβ are shown in orange and green sticks, respectively. Intramolecular hydrogen bonds are displayed as dotted lines. (**b**) Superposition of OGA_{cryst}–p53 complex structures collected from three independent soaking experiments (inserts: enlarged p53 glycopeptides from each monomer. The p53 glycopeptides in the right insert have been rotated for better clarity). (**c-d**) Close-up views of the binding conformations of p53 glycopeptides in (**c**) OGAα and (**d**) OGAβ. Residues on the inner surface of the substrate-binding cleft that are in close vicinity of the peptide are highlighted in (**c**) blue sticks and (**d**) yellow sticks, respectively. Hydrogen bonds are displayed in dashed lines. (**e**-**f**) Crystal packing potentially contributes to stabilize p53 glycopeptide in OGAβ but not in OGAα. OGAα and OGAβ are shown in magenta and yellow, respectively. The symmetric molecule is shown in grey.

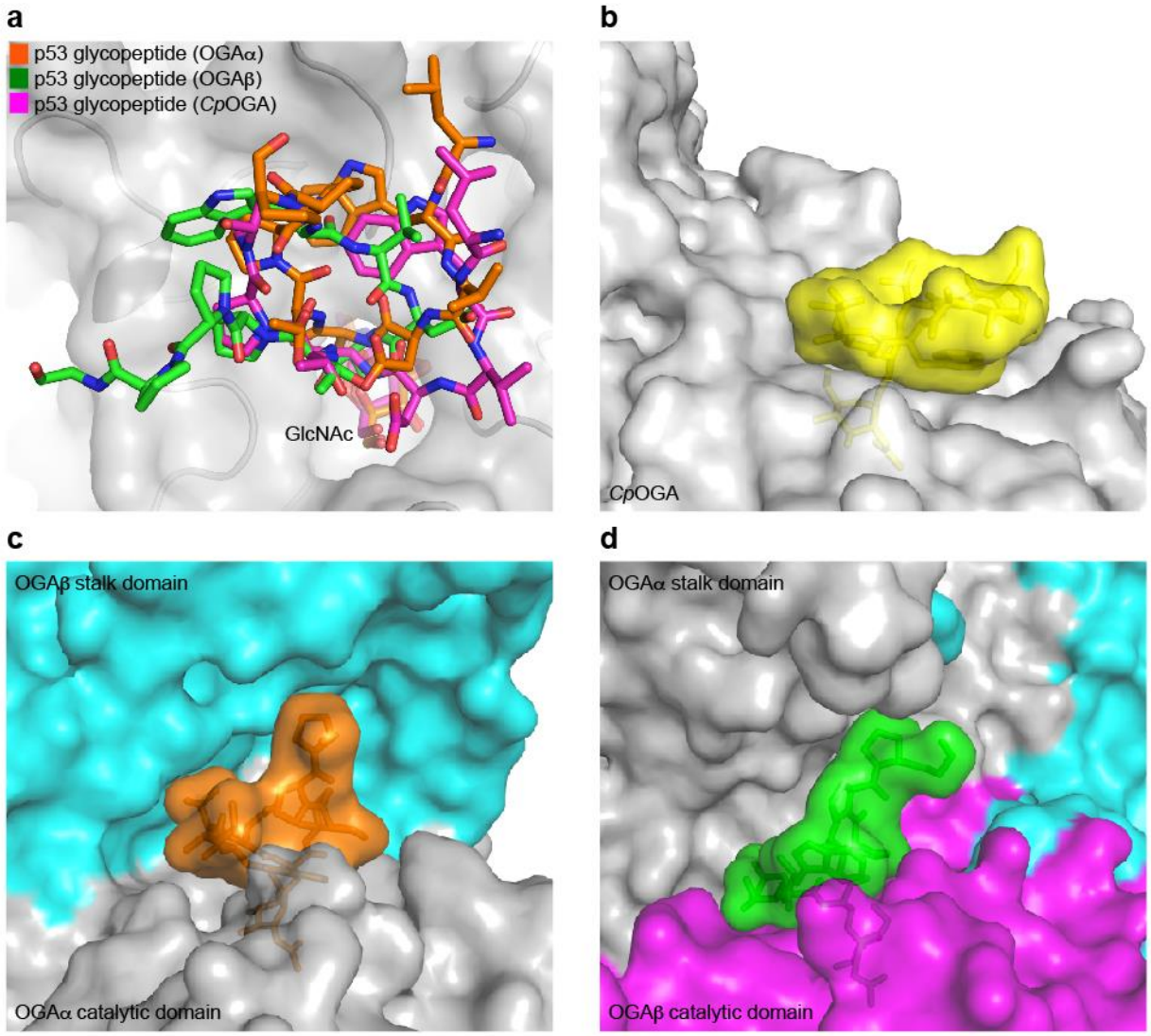

Supplementary Figure 8

The p53 glycopeptide adopts distinct binding conformations in the structures of human and bacterial OGAs.

(**a**) Superposition of the p53 glycopeptide (stick representation) in the *Cp*OGA–p53 complex (PDB: 2YDR) (Schimpl, M. *et al*., *Chem. Biol.* **19,** 173–178, 2012) with those in the OGA_{cryst}–p53 complex. (**b**) Surface representation of the *Cp*OGA–p53 complex, highlighting the p53 glycopeptide (yellow) bound on top of the active site (PDB: 2YDR). (**c**) Surface representation of the p53 glycopeptide (orange) bound in the substrate-binding cleft that comprises the catalytic domain of OGAα (grey) and the stalk domain of OGAβ (cyan). (**d**) Surface representation of the p53 glycopeptide (green) bound in the substrate-binding cleft that comprises the stalk domain of OGAα (grey) and the catalytic domain of OGAβ (magenta). In **b-d** panels, stick presentation of p53 glycopeptides is displayed as semitransparent.

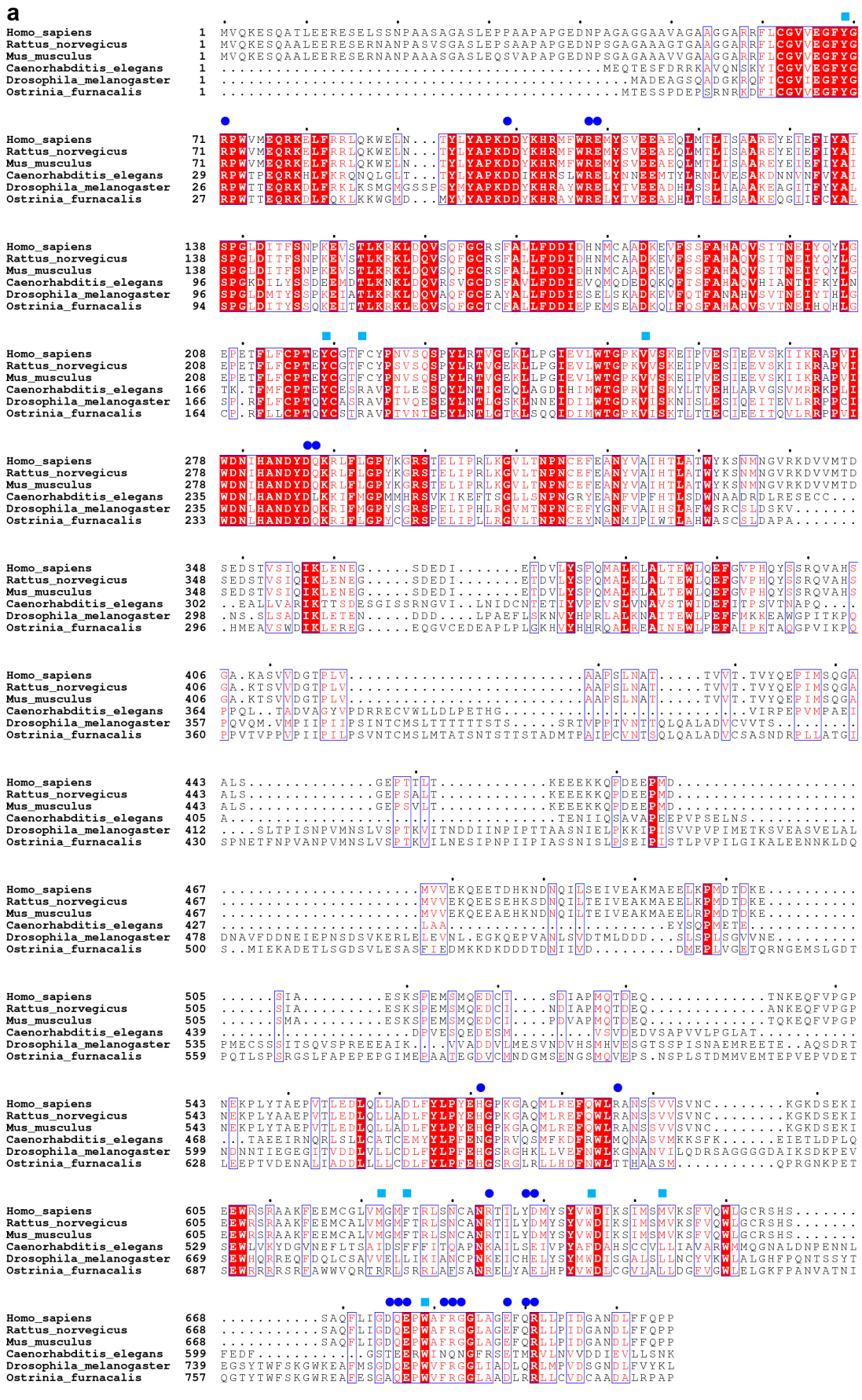
a
Homo_sapiens
Rattus_norvegicus
Mus_musculus
Caenorhabditis_elegans
Drosophila_melanogaster
Ostrinia_furnacalis

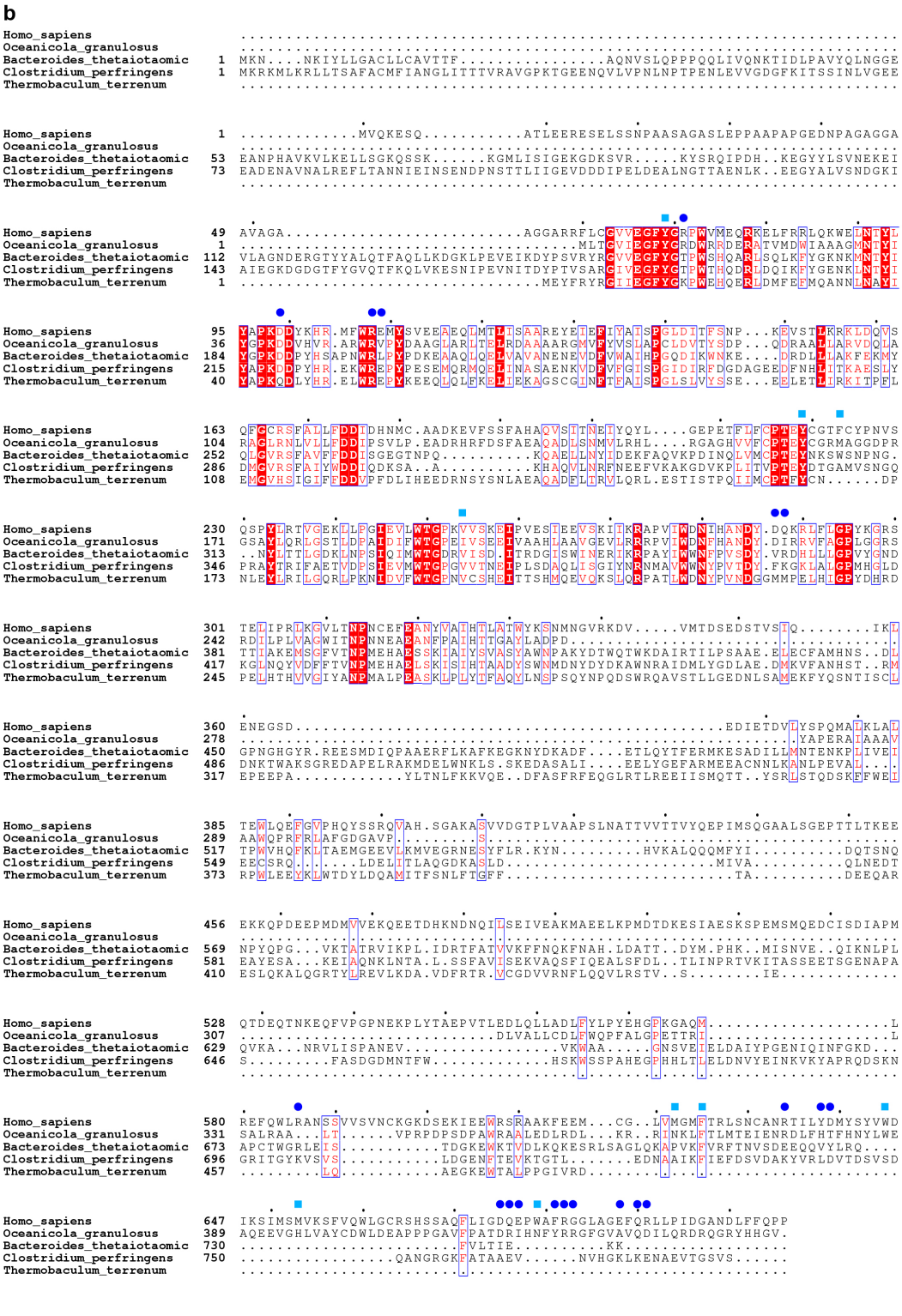

Supplementary Note 1

Sequence alignment of OGA proteins to show that residues on the dimerization interface and the substrate-binding cleft are highly conserved in eukaryotes but not in prokaryotes.

(**a**) Sequence alignment of OGA proteins from representative eukaryotic species: *Homo sapiens* (uniprot: O60502), *Rattus norvegicus* (uniprot: Q8VIJ5), *Mus musculus* (uniprot: Q9EQQ9), *Caenorhabditis elegans* (uniprot: A8WF17), *Drosophila melanogaster*, (uniprot: Q9VDC9), and *Ostrinia_furnacalis* (uniprot: H9NID4). (**b**)

Sequence alignment of OGA proteins from human and representative prokaryotic species: *Oceanicola granulosus* (uniprot: Q2CEE3), *Bacteroides thetaiotaomicron* (uniprot: Q89ZI2), *Clostridium perfringens* (uniprot: Q0TR53), and *Thermobaculum terrenum* (uniprot: D1CDN2). Variable residues are shown in black with white background, similar residues are shown in red with white background, and conserved residues are shown in white with red background. Residues involved in the dimerization of OGA_{cryst} are marked with dark blue dots. Hydrophobic residues on the substrate-binding cleft in close vicinity of the p53 glycopeptide are labeled by light blue squares.

Supplementary Table 1 A list of polar interactions between OGAα and OGAβ within 4 Å

OGAβ	Length (Å)	OGAα
Hydrogen bonds		
D99 [O]	3.0	Y638 [OH]
D99 [O]	3.0	R634 [NH1]
R108 [O]	3.4	S398 [OG]
E109 [OE]	2.8	Y397 [N]
E109 [OE2]	3.1	S398 [N]
D287 [OD2]	2.9	G683 [N]
Q288 [NE2]	2.8	S642 [OG]
R586 [NE]	2.7	L692 [O]
R634 [NH1]	2.9	D99 [O]
Y638 [OH]	3.0	D99 [O]
Q676 [O]	2.6	K253 [NZ]
E677 [OE1]	3.2	V255 [N]
E677 [OE2]	3.0	V254 [N]
F681 [O]	3.8	R290 [NH1]
R682 [O]	3.8	Q690 [NE2]
R682 [NH1]	2.9	Y286 [O]
G683 [N]	2.8	D287 [OD2]
E688 [OE2]	3.2	L701 [N]
Q690 [OE1]	2.8	K289 [NZ]
Salt bridges		
R71 [NH2]	3.2	D639 [OD1]
H571 [NE2]	2.7	E688 [OE1]
D639 [OD1]	3.0	R71 [NH2]
D675 [OD2]	2.8	K253 [NZ]
D675 [OD1]	3.8	K253 [NZ]
E688 [OE1]	2.7	H571 [NE2]
R691 [NE]	3.9	D696 [OD1]
R691 [NE]	4.0	D700 [OD2]
R691 [NH1]	2.5	D700 [OD1]
R691 [NH1]	2.9	D700 [OD2]

Supplementary Table 2 Summary of primers used to make OGA mutants in this study

Primer	Sequence (5′-3′)
K98A_fwd	ATACATACTTGTATGCCCCAGCAGATGACTACAAACATAGGATG
K98A_rev	CATCCTATGTTTGTAGTCATCTGCTGGGGCATACAAGTATGTAT
D174N_fwd	TGGGTGCAGATCATTTGCTTTGCTTTTTAATGATATAGACCATAATA
D174N_rev	TATTATGGTCTATATCATTAAAAAGCAAAGCAAATGATCTGCACCCA
D175N_fwd	GATCATTTGCTTTGCTTTTTGATAATATAGACCATAATATGTGTGCAGC
D175N_rev	CACATATTATGGTCTATATTATCAAAAAGCAAAGCAAATGATCTGCAC
Y219F_fwd	CTTCTGTCCCACAGAATTCTGTGGCACTTTCTGT
Y219F_rev	ACAGAAAGTGCCACAGAATTCTGTGGGACAGAAG
F223A_fwd	CCACAGAATACTGTGGCACTGCCTGTTATCCAAATGTGTCTC
F223A_rev	GAGACACATTTGGATAACAGGCAGTGCCACAGTATTCTGTGG
W278A_fwd	TTAAGAGAGCTCCAGTAATCGCGGATAACATTCATGCTAATG
W278A_rev	CATTAGCATGAATGTTATCCGCGATTACTGGAGCTCTCTTAA
D285A_fwd	CTGGGATAACATTCATGCTAATGCTTATGATCAGAAGAGACTGTTTC
D285A_rev	GAAACAGTCTCTTCTGATCATAAGCATTAGCATGAATGTTATCCCAG
W679A_fwd	GGAGACCAAGAACCCGCGGCCTTTAGAGGTGG
W679A_rev	CCACCTCTAAAGGCCGCGGGTTCTTGGTCTCC